Title
Light-Induced One Pot Synthesis for the Development of 89Zr-radiolabeled Antibodies

Author
Fong, Cyril Octavius Yu

Publication Date
2021

Peer reviewed|Thesis/dissertation

Light-Induced One Pot Synthesis for the Development of 89Zr-radiolabeled Antibodies

by
Cyril Octavius Yu Fong

THESIS
Submitted in partial satisfaction of the requirements for degree of
MASTER OF SCIENCE

in

Biomedical Imaging

in the

GRADUATE DIVISION
of the
UNIVERSITY OF CALIFORNIA, SAN FRANCISCO

Approved:

DocuSigned by:
45037357DBB24B1...
Henry F. VAnBrocklin
Chair

DocuSigned by:
Robert Flavell
Robert Flavell

DocuSigned by:
Michael Evans
Michael Evans

DocuSigned by:
Renuka Sriram
F54384405A42407...
Renuka Sriram

Committee Members

Acknowledgements

I dedicate this thesis to my family and friends, without whom this would have never been possible.

I would like to thank Dr. Henry VanBrocklin for accepting me as his student and providing me the opportunity to complete this project. I am thankful for my research mentors, Mr. Joseph Blecha and Dr. Kondapa Naidu Bobba for their assistance throughout my thesis project as well as sharing their invaluable knowledge to guide me in my academic career. Thank you to my committee members, Dr. Michael Evans, Dr. Robert Flavell, and Dr. Renuka Sriram, for providing support and advice throughout this process. I am extremely honored to have learned and worked alongside these marvelous individuals at UCSF.

I would like thank Dr. Jason Holland, Dr. Amaury Guillou, and Dr. Simon Klingler for their tremendous assistance and advice. Without them, I would not have had the materials and knowledge required for completing the project.

I would like to thank my family and friends, who have pushed and motivated me to continue chasing my dreams. Lastly, thank you to the 2021 MSBI Class for memories that I will always cherish.

Light-Induced One Pot Synthesis for the Development of ^{89}Zr-radiolabeled Antibodies

Cyril Fong

Abstract

Currently, the conventional synthesis of a radiolabeled VRC01 tracer to target the HIV reservoir in the human body is a two-step process. This process involves quality control tests of both the intermediate DFO-VRC01 conjugate and the ^{89}Zr-DFO-VRC01 product. A streamlined process could be made if characterization of the intermediate was eliminated by having the DFO chelate to the ^{89}Zr, followed by the immediate conjugation of the VRC01 by the ^{89}Zr-DFO. This method was explored by synthesizing ^{89}Zr-DFO-PEG$_3$-Azepin-mAb/protein using a light-induced one pot synthesis that could perform the radiolabeling and photoconjugation sequentially, bypassing the need to characterize an intermediate. **Methods:** A DFO-PEG$_3$-ArN$_3$ chelate was mixed with ^{89}Zr-oxalate to form ^{89}Zr-DFO-PEG$_3$-ArN$_3$, immediately followed by the addition of mAb/protein and irradiation by a 395 nm LED light. The crude reaction was purified using both PD-10 and G-100 size exclusion chromatography. The eluate obtained by the purification columns were analyzed by size exclusion HPLC. **Results:** The photoconjugation was successful for the synthesis of ^{89}Zr-DFO-PEG$_3$-Azepin-HSA, ^{89}Zr-DFO-PEG$_3$-Azepin-Cimzia, and ^{89}Zr-DFO-PEG$_3$-Azepin-VRC01. However, the photoconjugation conversion did not go to completion, resulting in ^{89}Zr-DFO-PEG$_3$-Azepin present in the crude reaction. Size exclusion PD-10 column purification gave inadequate separation of the ^{89}Zr-DFO-PEG$_3$-Azepin-mAb/proteins from ^{89}Zr-DFO-PEG$_3$-Azepin. G-100 column purifications significantly improved the separation of ^{89}Zr-DFO-PEG$_3$-Azepin-mAb/protein from ^{89}Zr-DFO-PEG$_3$-Azepin. However, the labeled Azepin was still present in smaller percentages. The binding assay conducted to determine immunoreactivity of ^{89}Zr-DFO-PEG$_3$-Azepin-VRC01 and ^{89}Zr-DFO-VRC01 gave

dissociation constants in the 0.4-20 nM range, comparable to previous findings. **Conclusion:** The photoconjugation method was successful in synthesizing ^{89}Zr-labeled HSA, Cimzia, and VRC01. The G-100 size exclusion column gave sufficient separation of ^{89}Zr-DFO-PEG$_3$-Azepin-mAbs/protein from ^{89}Zr-DFO-PEG$_3$-Azepin. The photoconjugation method did not affect the binding properties of ^{89}Zr-DFO-PEG$_3$-Azepin-VRC01 to the gp120 protein. Further work for more efficient photoconjugation and purification will be needed to foster future applications.

Table of Contents

List of Figures

List of Tables

Introduction

The utilization of proteins and monoclonal antibodies (mAbs) has led to a growing field of radioimmunotherapy (RIT) and Positron Emission Tomography (PET) tracer developments.[1] The increasing popularity for synthesizing mAb and protein-based radiotracers can be accredited to their versatile properties such as having high affinity and specificity towards its target protein, with desirable pharmacokinetics.[2] mAbs enable an exceptional tumor to non-tumor ratio when radiolabeled with biological half-life-compatible radioisotope,[3,4,8] which is a result of a faster distribution phase towards target specific antigens with a relatively slow elimination from the body that follow processes of proteolytic or lysosomal degradation.[5] Since mAbs are fairly large, with sizes ranging around 150 kDa, their movement is limited to interstitial spaces, with distribution being dependent on factors such as affinity to the target antigen and internalization.[4,5] The slow elimination of mAbs from the body allows for a longer half-life, therefore needing a radioisotope that could compliment the half-life of the mAb for imaging or therapy.[4,5]

Antibodies have been used to transport radioisotopes for imaging and therapy. Trastuzumab (Herceptin), developed at Genentech, was found to target the human epidermal growth factor receptor 2 (HER2) for the treatment of breast cancer.[6] Prior to the development of the antibody, HER2 expression was observed to vary in both primary and metastatic lesion, with the suggestion that multiple lesion biopsies to follow disease progression would be inadequate, as it was highly invasive.[6] This lead to the importance of utilizing molecular imaging to detect HER2 expression in individuals, which in comparison to biopsies, was minimally invasive.[6] Since then, trastuzumab has been radiolabeled for Single Photon Emission Computed Tomography (SPECT) and PET imaging as a first-line therapy and used in conjunction with

chemotherapy and radiation therapy.[6] Like trastuzumab, many mAbs have been created and radiolabeled with varying radioisotopes for different imaging modalities.

Given the long mAb biological half-life (days), it is important to use radioisotopes with physical half-lives that match the biological half-life.[7] Radioisotopes like those of ^{89}Zr ($t_{1/2}$: 78.4 hr), ^{64}Cu ($t_{1/2}$: 12.7 hr), ^{123}I ($t_{1/2}$: 13.2 hr) and ^{111}In ($t_{1/2}$: 67.2 hr) have been used to radiolabel mAb/protein-based diagnostic tracers for PET and SPECT imaging.[2] Of the radioisotopes used in PET imaging, ^{89}Zr has emerged as the isotope of choice. The push in using ^{89}Zr as compared to its predecessors can be attributed to its physical half-life, matching the biological half-life of an antibody as compared to the half-lives of ^{86}Y and ^{64}Cu.[7,8] When compared to ^{124}I, ^{89}Zr emits lower energy positrons which provides greater spatial resolution, does not dehalogenate in vivo, and does not have a complicated decay schema that could result in poor image resolution.[7,8]

With ^{89}Zr placed into the class of "hard cation" due to its strong 4+ cationic state, there is a preference to coordinate with compounds bearing eight or less anionic oxygen donors, like the commonly used siderophore, desferrioxamine (DFO), seen in Figure 1.[8] The binding of DFO to ^{89}Zr is strong because of the bond formed between the 3 hydroxamate groups of the DFO, along with three neutral oxygen bonds and two water bonds.[8,9]

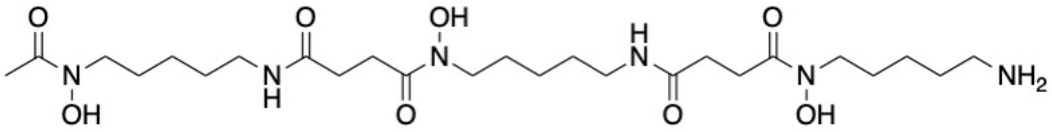

Figure 1: Structure of desferrioxamine. The siderophore, desferrioxamine (DFO), is commonly used to chelate ^{89}Zr because of the strong cationic bond between the ^{89}Zr and hydroxamate groups.

The commonly used derivative of DFO to chelate ^{89}Zr is *p*-isothiocyanatobenzyl-desferrioxamine (*p*-DFO-SCN) (1).[9] Currently, the FDA compliant method of synthesizing ^{89}Zr-labeled mAb involves a two-step step process as seen below in Figure 2.

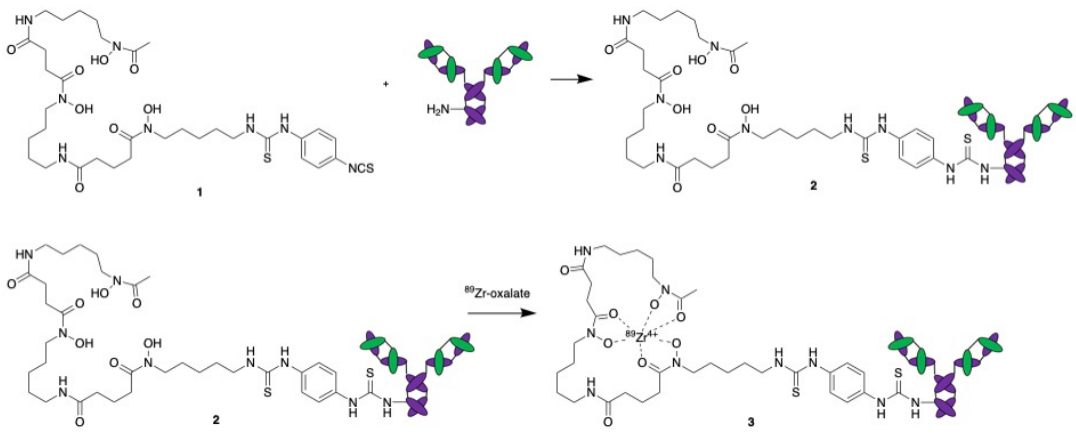

Figure 2: Synthesis of ^{89}Zr-DFO-mAb. The DFO-chelate (1) is conjugated to the mAb/protein (2), followed by radiolabeling to produce 89Zr-DFO-mAb/protein (3).

The starting DFO-chelate, 1, is conjugated to the mAb/protein, producing a DFO-mAb/protein intermediate, 2. Before being radiolabeled with ^{89}Zr, 2 would first undergo a set of quality control tests to determine the compounds appearance, monomer content, pH, endotoxin content, concentration, chelate to protein binding, sterility, and radiochemical purity.[10,11] If the intermediate successfully passes all the quality control tests, it will be ready for radiolabeling. The DFO-mAb, 2, is radiolabeled with ^{89}Zr-oxalate, producing ^{89}Zr-DFO-mAb, 3. Before being administered to the patient, 3 must undergo pre-release and post release quality control tests. The pre-release testing determines the radio-tracer's radiochemical purity, appearance, pH, endotoxin content, and filter integrity.[10] The post-release testing determines the radio-tracer's binding and sterility. After passing these quality control tests will ^{89}Zr-DFO-mAb be administered to a patient.

The cGMP is a system enforced by the FDA to regulate facilities and their manufacturing processes. Specifications for the PET agent must be established, which includes determining the identity, quality, purity, pyrogens, sterility, and strength.[10,11] As per the standard of procedure (SOP) for the full characterization of DFO-mAb, requires a sterility test of the intermediate is conducted for 14 days.[10] The intermediate is inoculated in two growth medias, Tryptic Soy Broth

(TSB) and Fluid Thioglycollate Medium (FTM) and incubated at two different temperatures to promote the growth of bacteria.[10] At the end of 14 days of incubation, if bacterial growth is observed in either solution, this would be indicative of a non-sterile product.[10] This current process requires quality testing of the intermediate and final product. This process could be streamlined if the intermediate quality control testing could be eliminated. The only way to do that is if the conjugation of the chelate to the antibody and the ^{89}Zr chelation to the DFO occurred in a single step.

The goal of the current project was to utilize a previously developed light-induced one-step synthesis that would perform a radiolabeling and conjugation simultaneously. This is advantageous because it bypasses the need for a full characterization of the intermediate, 2 during the synthesis of the radiotracer to be administered in the clinical setting.[2] A schematic for the synthesis as well as the reaction setup is shown in Figure 3. The DFO-PEG$_3$-ArN$_3$ chelate, 4, is first radiolabeled with ^{89}Zr-oxalate, to produce ^{89}Zr-DFO-PEG$_3$-ArN$_3$, 5. The mAb/protein is added a couple minutes after mixing, and a 395nm LED light is turned on for 15 minutes to allow for photoconjugation, forming ^{89}Zr-DFO-PEG$_3$-Azepin-mAb/protein, 6.

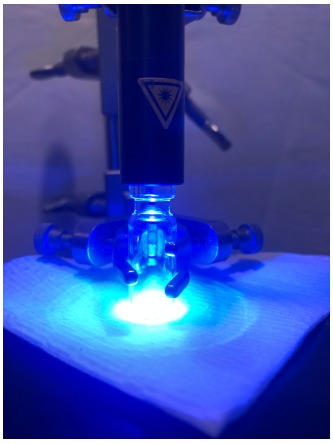

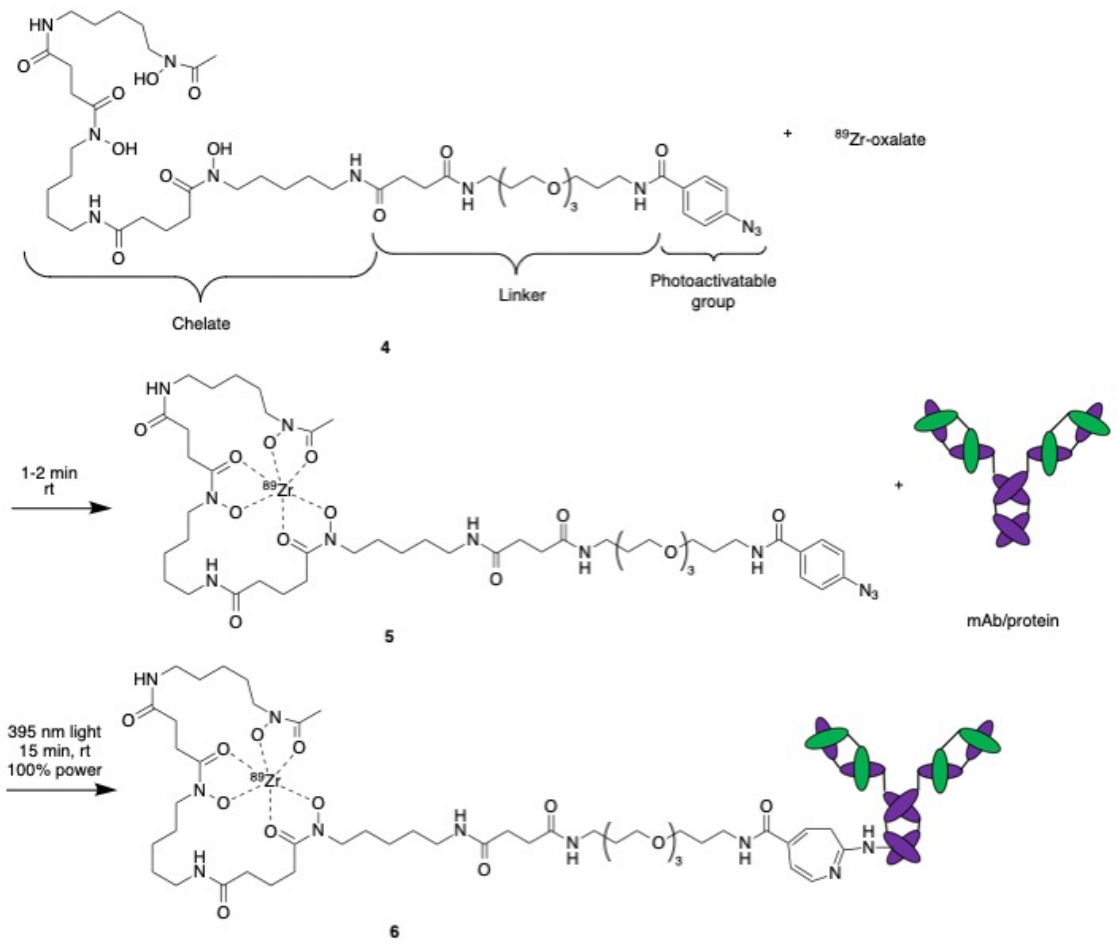

Figure 3: Reaction Setup and One Pot Synthesis. (Top) The reaction setup for the light-induced synthesis. (Bottom) Synthesis of ^{89}Zr-DFO-PEG$_3$-Azepin-Ab/protein utilizing a light induced reaction at room temperature.

Two mAbs and a protein were used to evaluate this photoconjugation process. The protein, Human Serum Albumin (HSA), is a plasma protein that has been previously radiolabeled with ^{131}I and ^{18}F for angiography and blood-pool imaging.[12] HSA was used because it was readily available, inexpensive, and has been successfully synthesized by our collaborators at the University of Zurich, providing reference data for comparison. The first mAb, certolizumab, is an anti-tumor necrosis factor (anti-TNFα) inhibitor that has been labeled with longer lived radioisotopes like ^{89}Zr for the evaluation of anti-TNFα therapeutics delivery.[13] Cimzia was used because it was also readily available. The second mAb used to validate the

photoconjugation process was VRC01, a mAb from a class of bNAbs that interact with the gp120's CD4 binding site region.[14,15] VRC01 has been used to treat HIV-1 infected patients by neutralizing more than 80% of the HIV-1 strain, preventing the further spread of the virus.[14,15] The mAb had been successfully radiolabeled with ^{89}Zr at UCSF and has shown potential in identifying and quantifying persistent HIV in patients undergoing antiretroviral therapy (ART) through PET/MR.[16]

Methods

A. Materials

Chemicals were purchased from the following vendors: Spectrum Chemical MFG, Sigma Aldrich, Alfa Aesar, and were used as received. p-DFO-SCN (Macrocyclics, Dallas, Texas), VRC01 (NIH Vaccine Research Center, Bethesda, Maryland), ^{89}Zr-oxalate (3D Imaging, Little Rock, AR), and DFO-PEG3-Azide (Holland Lab at the University of Zurich, Zürich, Switzerland).

The light source for the photoconjugation reaction was an Opsytec Dr. Groebel LedControl S with a 395 nm LED light under the following parameters: Power = 100%, duration = 15 minutes, Activation = trigger. Size exclusion column high performance liquid chromatography (SEC-HPLC) analysis were performed on a Hitachi LaChrom Elite with the following parameter: Flow rate = 1.0 mL/min using the software, EZChrom Elite. Two size exclusion HPLC columns were used, i) a Biosep 5mm SEC-s3000 290Å 300 x 7.8 mm and ii) a BioRad ENrich SEC 650 300 x 10 mm. Ultraviolet (UV) detection was performed on a Shimazu SPD-UV detector at 280 nm and in-line gamma radiation detection using a Carroll & Ramsey flow detector (Model 105s, Berkeley, CA) with data collected by SRI PeakSimple software (Torrance, CA). Instant thin layer chromatography (iTLC) analysis was performed on a BioScan

AR-2000 using the software, WinScan V3. Concentrations were determined using a Thermo Scientific Nanodrop One. Binding curves were generated using the software, GraphPad Prism (GraphPad Software Inc., La Jolla, CA). Radioactivity was measured using a Hidex AMG (Finland) counter.

B. DFO-VRC01

To a 2.0 mL centrifuge tube, 20 µL of a 25mg/mL p-DFO-SCN stock solution and 1 mL of 0.1M $NaHCO_3/Na_2CO_3$ pH 9 were added and mixed. In a 1.5 mL tube, 100 µL of VRC01 was added to 500 µL of 0.1M $NaHCO_3/Na_2CO_3$ pH 9. To another 1.5 mL tube, 300 µL of the DFO-p-SCN/ $NaHCO_3/Na_2CO_3$ was added to 600 µL VRC01/ $NaHCO_3/Na_2CO_3$. The reaction mixture was incubated at 37°C for 45 minutes with gentle stirring. The DFO-VRC01 conjugate was purified by size exclusion chromatography using a PD-10 desalting column with a 0.25M sodium acetate trihydrate solution serving as the eluent.

The full reaction volume (1 mL) was added to the center of the top frit and collected. The reaction vial was rinsed with 1 mL 0.25M NaOAc•3H2O/Gentisic Acid and the 1 mL was added to the center of the top frit and collected. Another 1 mL of 0.25M NaOAc•3H2O/Gentisic Acid was added to the top and allowed to be collected. This was repeated for four more fractions. The concentration of purified product was measured using a Nanodrop One three times using 2 µL aliquots. The purity of the compound was determined using SEC-HPLC. The purified conjugate (20 µL) was injected into a BioSep 5 µm SEC-s3000 290 Å 300 x 7.8 mm column twice. The mobile phase used was a PBS solution with a steady flow rate of 1 mL/min.

C. ^{89}Zr-DFO-VRC01

In a 2-mL tube containing 20 µL of deionized H_2O, 2.02 mCi (4.4 µL) of ^{89}Zr-oxalate and an equivalent volume of 1M Na_2CO_3 were added and incubated at room temperature for 3

minutes. To the tube containing the neutralized ^{89}Zr, 2 mg (297.5 µL) of DFO-VRC01 from a 6.723 mg/mL stock dissolved in 673.7 µL of 1M ammonium acetate were added. The reaction was incubated for 1 hour at room temperature with gentle mixing. The product was purified using a PD-10 column with 0.25M NaOAc•3H2O/Gentisic Acid serving as the eluent.

The full reaction volume (1 mL) was added to the center of the top frit and collected. The reaction vial was rinsed with 1 mL 0.25M NaOAc•3H2O/Gentisic Acid and the 1 mL was added to the center of the top frit and collected. Another 1 mL of 0.25M NaOAc•3H2O/Gentisic Acid was added to the top and allowed to be collected. Lastly, 2 mL of 0.25M NaOAc•3H2O/Gentisic Acid was added to the top and allowed to be collected. Fractions of 1 mL were collected, and the radioactivity was measured using a dose calibrator. Radiolabeling efficiency of the reaction was determined using instant iTLC. An aliquot (1 µL) of the radiolabeled compound was spotted on a glass microfiber chromatography paper impregnated with silicic acid and added to a 50-mL tube containing 10 mL of 50mM diethylenetriamine pentaacetic acid (DTPA). The radiochemical purity was measured using HPLC by observing the UV and radioactivity signals using a 20 µL injection of the purified product. The mobile phase used was 0.05M Na_2HPO_4/NaH_2PO_4 solution containing 250 µg/mL of NaN_3 with a steady flow rate of 1.0 mL/min.

D. ^{89}Zr-DFO-PEG$_3$-Azepin-Ab/protein

In a vial containing 98.5 µL of water and a stir bar, 22.5 nmol (10.6 µL) of DFO-PEG$_3$-Azide followed by 2 mCi (2.6 µL) of ^{89}Zr-oxalate and an equivalent volume of 1M Na_2CO_3 were added and mixed for 2 minutes at room temperature. Radiolabeling efficiency of the reaction was determined using iTLC. An aliquot (1 µL) of the radiolabeled compound was spotted on a glass microfiber chromatography paper impregnated with silicic acid and added to a 50-mL tube containing 10 mL of DTPA. The radiochemical purity was measured using HPLC by observing

the UV and radioactivity signals using a 10 µL injection of the radiolabeled product. The mobile phase used was 0.05M Na_2HPO_4/NaH_2PO_4 solution containing 250 µg/mL of NaN_3 with a steady flow rate of 1.0 mL/min.

After 2 minutes of mixing, 15 nmol of Ab/protein are added to the reaction vial. The Ab/proteins used for the photoconjugation reaction were VRC01, HSA, and Cimzia. The reaction vessel was then irradiated using a 395 nm LED light for 15 minutes at 100% power. Photoconjugation efficiency was determined using HPLC by observing UV and radioactivity signals using a 10 µL injection of the reaction solution.

E. PD-10 Purification

The reaction volume (120 µL) was added to the center of the top frit and collected in the first fraction. An addition of 1 mL 0.25M NaOAc•3H2O/Gentisic Acid was added to the center of the top frit and collected in the same fraction. The addition and collection of 1 mL fractions totaled eight fractions. The radioactivity was measured using a dose calibrator. The radiochemical purity was measured using HPLC by observing the UV and radioactivity signals using a 100 µL injection of the purified product. The mobile phase used was 0.05M sodium phosphate monobasic/sodium phosphate dibasic solution containing 250 µg/mL of sodium azide with a steady flow rate of 1.0 mL/min.

F. Sephadex G-100 Column Purification

A frit was inserted and placed at the bottom of an empty PD-10 column. A solution of 1x PBS (1 mL) was added to the column, followed by the addition of Sephadex G-100 (431.5 mg). The Sephadex powder was further dissolved in 3 mL of 1x PBS, followed by a vortexing of the solution. The column was filled with 5 mL of 1x PBS, capped, and allowed to sit for five days in a 12-14°C fridge. The reaction volume (120 µL) was added to the center of the top frit and

collected. An addition of 80 µL PBS was added to the center of the top frit and collected in the same fraction. The addition and collection of 200 µL fractions totaled 40 fractions.

G. Biological Activity Assay

Dilution of Labeled VRC01 Analogs

Into a microtube labeled 1, 375 µL of 1% nonfat milk and 125 µL of ^{89}Zr-DFO-VRC01 or ^{89}Zr-DFO-PEG$_3$-Azepin-VRC01were added and mixed. In microtubes labeled 2-8, 400 µL of 1% nonfat milk were added. From microtube 1, 100 µL of solution was taken out and added to microtube 2. The following dilution process was done with microtubes 3-8.

Coating of 96-well Enzyme-Linked Immunosorbent Assay (ELISA) Plate

In a clean 96-well ELISA plate, 100 µL of 5 µg/mL Resurfaced Stabilized Core (RSC3) was added in 32 wells: Rows A-H and columns 1-3. The plate was sealed with an adhesive plate sealer and incubated at 4°C for 24 hours.

Incubation of ELISA Plate

After incubation, the plate was allowed to equilibrate to room temperature. The liquid was aspirated from each well and discarded. A solution of 0.5% PBS-Tween (150 µL) was added to each well, followed by an agitation of the plate for 2 minutes, followed by an aspiration of the liquid. This process was repeated two more times. A 1% nonfat milk solution (150 µL) was added to each well, followed by a sealing of the plate and incubation for 1 hour at room temperature.

Incubation of Labeled VRC01 Analogs and Processing

Following the incubation, the liquid in each well was aspirated and discarded. From microtube 1, 100 µL of solution was added to the three wells in row A. The same procedure was

followed for each microtube 2-8, adding to rows B-H. The ELISA plate was then incubated for 1 hour at room temperature.

The liquid in each well was aspired and discarded. A solution of 0.5% PBS-Tween (150 µL) was added to each well, followed by an agitation of the plate for 2 minutes, followed by an aspiration of the liquid. This process was repeated two more times. A solution of 1M NaOH (200 µL) was added to each well and the plate was incubated at room temperature for 25 minutes. The liquid in each well is aspirated and placed into 24 tubes. The activity counts for each sample were measured for 30 seconds using a gamma counter (Hidex). Statistical analyses were performed using GraphPad Prism (GraphPad Software Inc., La Jolla, CA).

Results

A. Conventional Synthesis

^{89}Zr-DFO-VRC01

DFO-VRC01 was prepared by conjugating VRC01 with p-DFO-SCN at room temperature. The conjugate was purified through a size exclusion PD-10 column using a 0.25M NaOAc•3H_2O eluent and collected in 1 mL fractions. The concentration of DFO-VRC01 in fractions 4, 5, and 6 were measured on a NanoDrop. The purified DFO-VRC01 in fraction 4 was 0.535 mg/mL, in fraction 5 was 6.723 mg/mL, and in fraction 6 was 1.024 mg/mL. Fraction 5 was used in the subsequent reactions.

DFO-VRC01 was radiolabeled with neutralized ^{89}Zr-oxalate at room temperature for half an hour. The radiolabeling efficiency, as measured by iTLC, demonstrated complete chelation of ^{89}Zr with the peak retained at the origin and no free ^{89}Zr. An iTLC of ^{89}Zr-oxalate was performed to show the movement of free ^{89}Zr up the iTLC plate. Both iTLC chromatograms are seen in Figure 4.

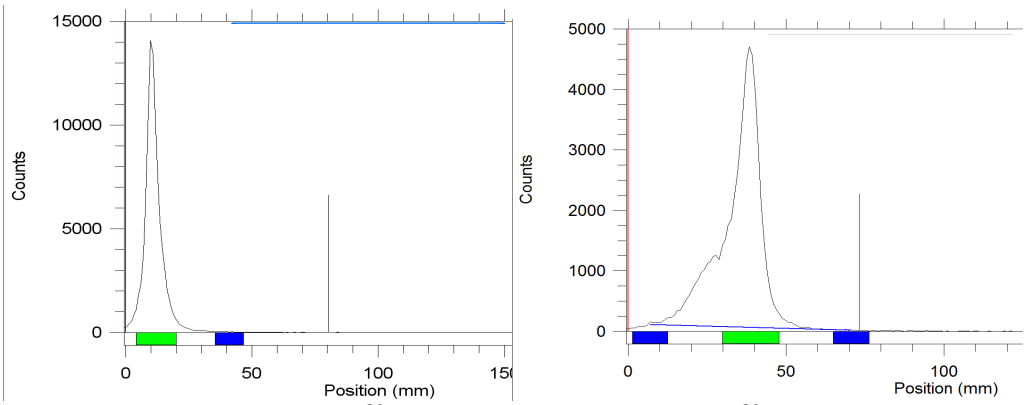

Figure 4: iTLC chromatograms of ^{89}Zr-DFO-VRC01 and free ^{89}Zr. The left chromatogram of ^{89}Zr-DFO-VRC01 indicating complete radiolabeling based on the single peak retained at the origin containing 100% of counts within the region. The right chromatogram of ^{89}Zr-oxalate shows retention along solvent front.

Radiolabeled ^{89}Zr-DFO-VRC01 was purified through a size exclusion PD-10 column using a 0.25M NaOAc•3H_2O/Gentisic Acid eluent and collected in 1 mL fractions. A typical elution profile from a 2 mCi reaction was generated with the activity observed in each fraction, shown in Figure 5. Analysis of the elution profile showed that ^{89}Zr-DFO-VRC01 eluted into fractions 3 to 6. A majority of ^{89}Zr-DFO-VRC01 eluted into fractions 4 and 5.

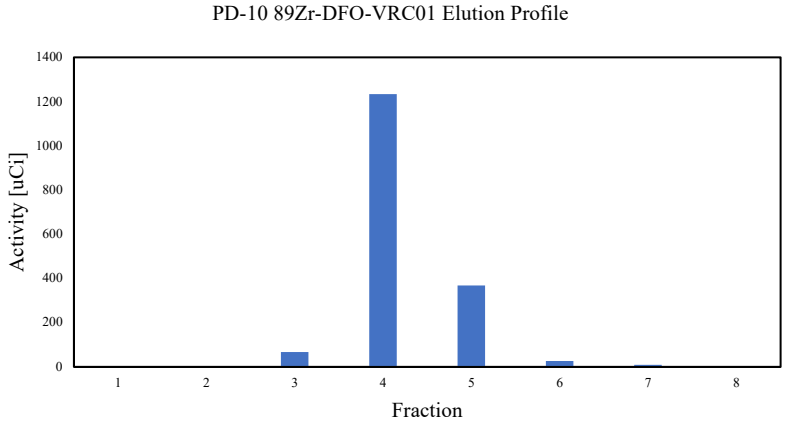

Figure 5: PD-10 ^{89}Zr-DFO-VRC01 elution profile. The elution profile of ^{89}Zr-DFO-VRC01 from the fractions of activity eluted from a PD-10 column.

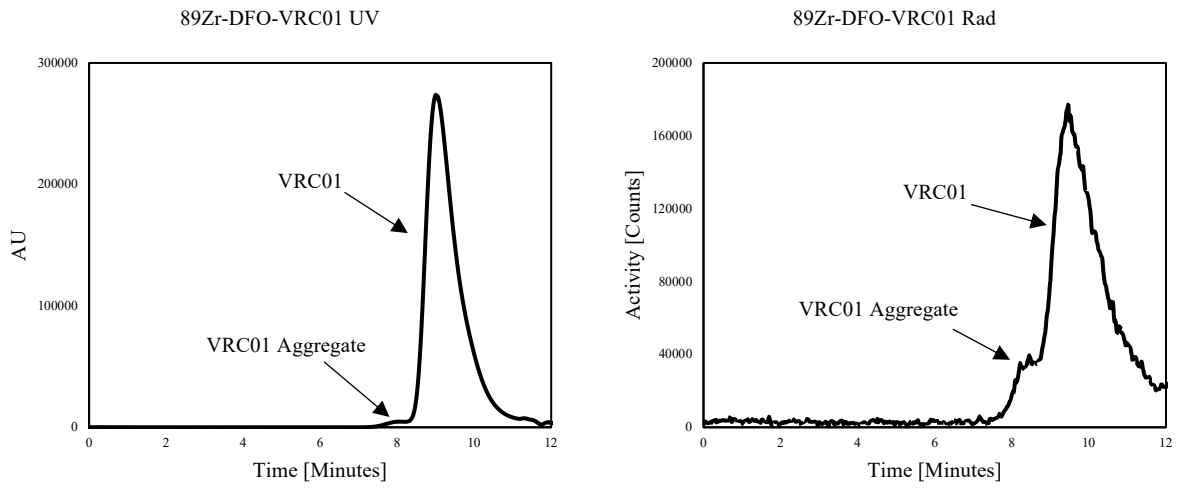

Figure 6: UV/Rad chromatograms of ^{89}Zr-DFO-VRC01. The UV (left) and radiation (right) chromatograms of ^{89}Zr-DFO-VRC01. The major species is ^{89}Zr-DFO-VRC01 seen at 9.5 minutes with the minor species being the aggregate at 8.4 minutes. The UV chromatogram shows ^{89}Zr-DFO-VRC01 at 9.1 minutes with its lower molecular weight aggregate at 9.1 minutes.

The radiochemical purity of ^{89}Zr-DFO-VRC01 was analyzed by HPLC with UV/Radiation detection using a Biosep 5mm SEC-s3000 290Å size exclusion column eluted with a Na_2HPO_4/NaH_2PO_4/Gentisic Acid mobile phase seen in Figure 6. A majority of ^{89}Zr-DFO-VRC01 elutes from the HPLC column at 9.5 minutes with the higher molecular weight aggregate peak at 8.4 minutes. The corresponding UV chromatogram showed ^{89}Zr-DFO-VRC01 peaking at 9.1 minutes with the aggregate peak at 8.1minutes. The amount of monomer was 91.5%. The amount of high molecular weight species in the fraction was 8.5%. No low molecular weight species were detected so the radiochemical purity was 91.5%.

A binding assay was performed to assess the immunoreactivity of the labeled VRC01 by conducting eight five-fold dilutions of the purified ^{89}Zr-DFO-VRC01 in triplicate. The diluted radiolabeled VRC01 was incubated with a RSC3 recombinant protein for two hours. The activity of extracted protein was measured on a Hidex gamma counter, and a binding curve was generated, shown in Figure 7. The dissociation constant of ^{89}Zr-DFO-VRC01 was calculated as 19.72 ± 2.998 nM and $R^2 = 0.9981$.

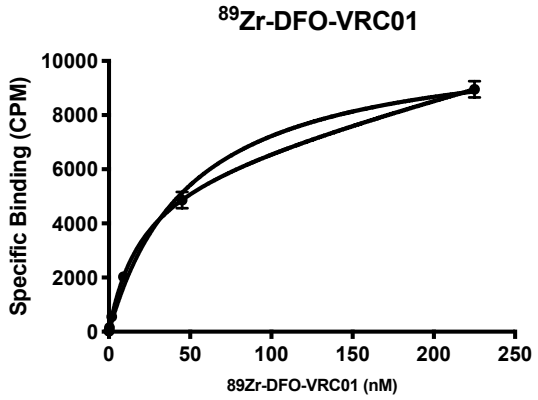

Figure 7: Biological activity assay of ^{89}Zr-DFO-VRC01. The dissociation constant of ^{89}Zr-DFO-VRC01 to a RSC3 recombinant protein. K_D for ^{89}Zr-DFO-VRC01 is 19.72 ± 2.998 nM (n = 3, R^2 = 0.9981).

B. Photoconjugation

^{89}Zr-DFO-PEG$_3$-ArN$_3$

DFO-PEG$_3$-ArN$_3$ was radiolabeled with neutralized ^{89}Zr-oxalate at room temperature for two minutes. As seen in Figure 8, the radiolabeling efficiency measured by iTLC, was 100%.

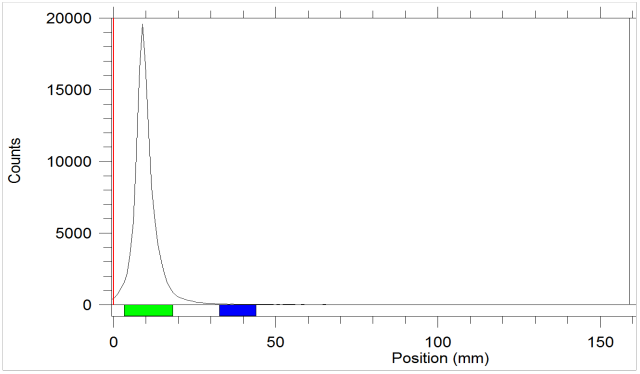

Figure 8: iTLC of ^{89}Zr-DFO-PEG$_3$-ArN$_3$. The chromatogram of ^{89}Zr-DFO-PEG$_3$-ArN$_3$ indicating complete radiolabeling based on the single peak retained at the origin containing 100% of counts within the region.

The radiochemical purity of ^{89}Zr-DFO-PEG$_3$-ArN$_3$ was analyzed by HPLC with UV/Radiation detection using a Biosep 5mm SEC-s3000 290Å size exclusion column eluted with a PBS mobile phase, seen in Figure 9. The radiation chromatogram showed ^{89}Zr-DFO-

PEG_3-ArN_3 at 19.2 minutes. The corresponding UV chromatogram showed ^{89}Zr-DFO-PEG_3-ArN_3 at 18.9 minutes. These chromatograms confirm the iTLC results.

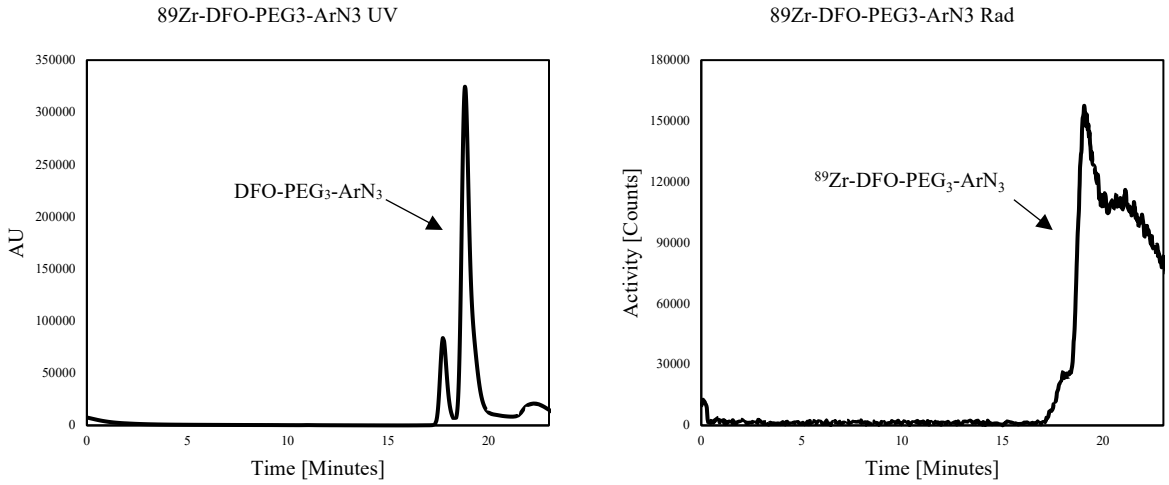

Figure 9: UV/Rad chromatogram of ^{89}Zr-DFO-PEG_3-ArN_3. The UV (left) and radiation (right) chromatograms of ^{89}Zr-DFO-PEG_3-ArN_3. The major species is ^{89}Zr-DFO-PEG_3-ArN_3 seen at 19.2 minutes. The UV chromatogram shows ^{89}Zr-DFO-PEG_3-ArN_3 at 18.9 minutes.

^{89}Zr-DFO-PEG_3-Azepin-HSA

Following the ^{89}Zr-DFO-PEG_3-ArN_3 radiolabeling, HSA was added and the reaction was irradiated for 15 minutes at room temperature to synthesize ^{89}Zr-DFO-PEG_3-Azepin-HSA, a model protein compound. The radiochemical purity of the crude ^{89}Zr-DFO-PEG_3-Azepin-HSA was analyzed by HPLC with UV/Radiation detection using a Biosep 5mm SEC-s3000 290Å size exclusion column eluted with a PBS mobile phase is shown in Figure 10. Analysis of the radiation chromatogram shows a majority of ^{89}Zr-DFO-PEG_3-Azepin-HSA at 9.8 minutes. The minor species being the ^{89}Zr-DFO-PEG_3-Azepin at 11.3 minutes.

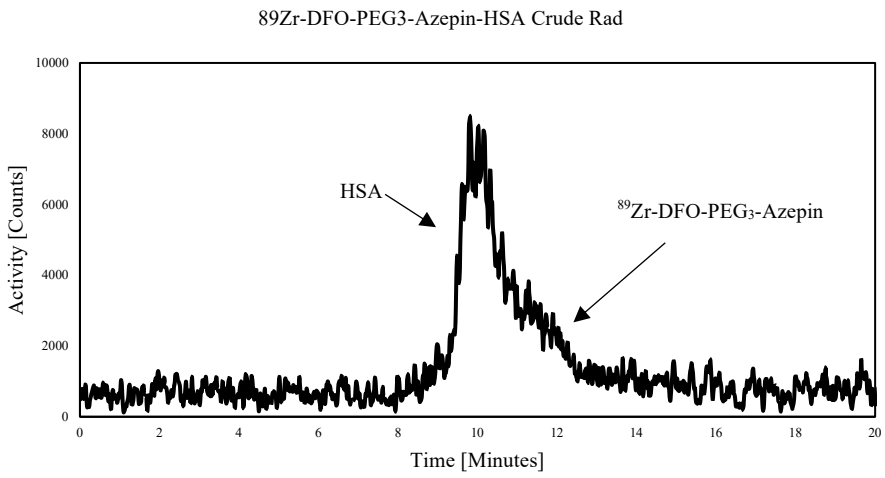

Figure 10: Rad chromatogram of crude ^{89}Zr-DFO-PEG$_3$-Azepin-HSA. The major species is ^{89}Zr-DFO-PEG$_3$-Azepin-HSA seen at 9.8 minutes and the minor species is ^{89}Zr-DFO-PEG$_3$-Azepin seen at 11.8 minutes.

The crude reaction was purified through a PD-10 column using a 0.25M NaOAc•3H_2O/Gentisic Acid eluent and collected in 1 mL factions. A typical elution profile from a 257 μCi reaction was generated and compared to the elution profile of ^{89}Zr-DFO-PEG$_3$-Azepin, shown in Figure 11. It was observed that ^{89}Zr-DFO-PEG$_3$-Azepin-HSA eluted into fractions 3 to 8. A majority of the activity eluted into fractions 3 and 4. The elution profile for ^{89}Zr-DFO-PEG$_3$-Azepin showed that the compound had eluted into fractions 4 to 8, with a majority eluting into fractions 5 to 7. It appears that the labeled HSA and remaining Azepin may overlap and coelute in a few fractions.

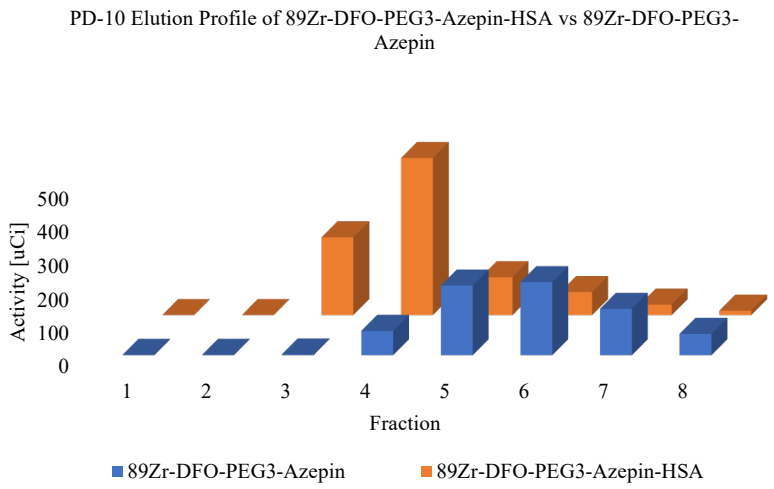

Figure 11: PD-10 fractions of ^{89}Zr-DFO-PEG$_3$-Azepin-HSA/^{89}Zr-DFO-PEG$_3$-Azepin. The elution profiles are compared to show the overlap of species in the ^{89}Zr-DFO-PEG$_3$-Azepin-HSA fractions.

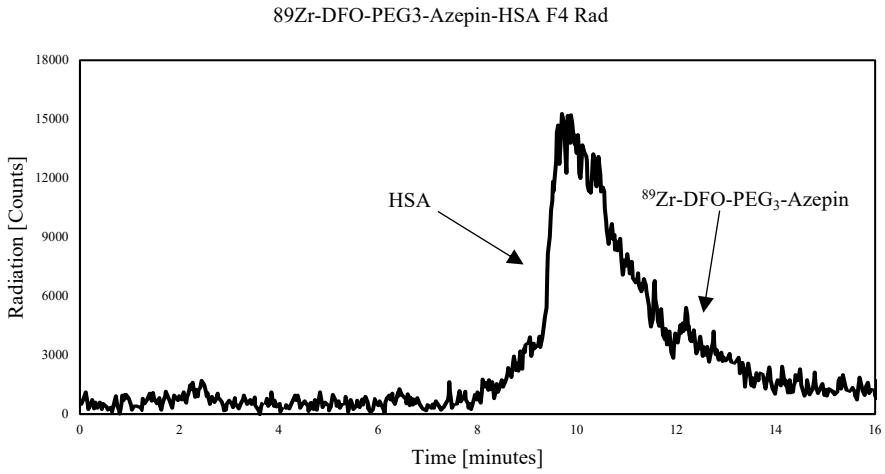

Figure 12: Rad chromatogram of ^{89}Zr-DFO-PEG$_3$-Azepin-HSA F4. The major species is ^{89}Zr-DFO-PEG$_3$-Azepin-HSA seen at 9.8 minutes and the minor species is ^{89}Zr-DFO-PEG$_3$-Azepin seen at 11.8 minutes.

The purity of ^{89}Zr-DFO-PEG$_3$-Azepin-HSA in fraction 4 was analyzed by HPLC with UV/Radiation detection using a Biosep 5mm SEC-s3000 290Å size exclusion column eluted with a Na_2HPO_4/NaH_2PO_4/Gentisic Acid mobile phase seen in Figure 12. The chromatogram of the "purified fraction' appears to have residual ^{89}Zr-DFO-PEG$_3$-Azepin present.

A subsequent HSA reaction was purified through a Sephadex G-100 column using a PBS eluent and collected in 200 µL fractions. An elution profile, shown in Figure 13, of a 2 mCi reaction was generated. Two distinct peaks were observed, the first peak between fractions 10 and 20, and the second between fractions 25 and 40.

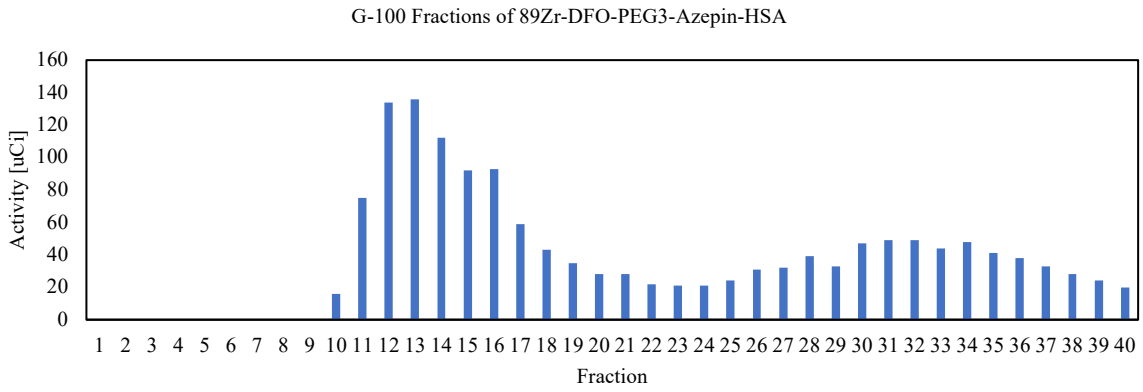

Figure 13: G-100 elution profile of ^{89}Zr-DFO-PEG$_3$-Azepin-HSA. There are two distinct peaks. The first peak, ^{89}Zr-DFO-PEG$_3$-Azepin-HSA, resides between fractions 10 and 20, and the second peak, ^{89}Zr-DFO-PEG$_3$-Azepin, resides between fractions 25 and 40.

The crude and G-100 purified ^{89}Zr-DFO-PEG$_3$-Azepin-HSA were analyzed by HPLC with UV/Radiation detection using a BioRad ENrich SEC 650 size exclusion column eluted with a PBS mobile phase, shown in Figure 14. The HPLC chromatogram of the crude reaction shows that the reaction did not completely form ^{89}Zr-DFO-PEG$_3$-Azepin-HSA. The percent photoconjugation was 55.0%. The HPLC of fraction 13 from the G-100 purification showed ^{89}Zr-DFO-PEG$_3$-Azepin-HSA as the major species with 6.5% of ^{89}Zr-DFO-PEG$_3$-Azepin. This demonstrates that the G-100 column does not completely separate ^{89}Zr-DFO-PEG$_3$-Azepin-HSA from the ^{89}Zr-DFO-PEG$_3$-Azepin.

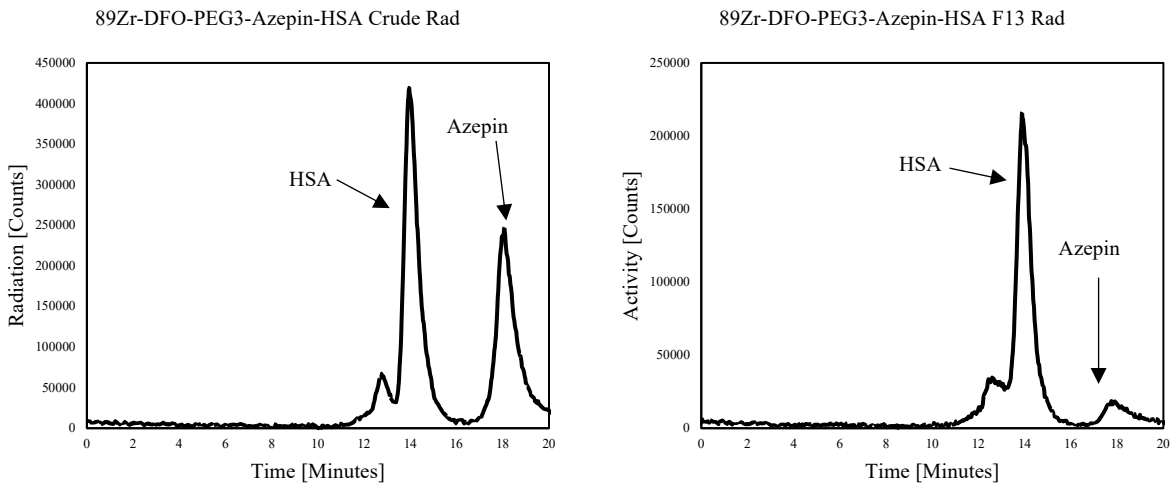

Figure 14: Rad chromatogram of crude and G-100 purified ^{89}Zr-DFO-PEG$_3$-Azepin-HSA. The radiation chromatograms of the crude ^{89}Zr-DFO-PEG$_3$-Azepin-HSA (left) and G-100 purified ^{89}Zr-DFO-PEG$_3$-Azepin-HSA fraction 13 (right). The major species in both the crude reaction and fraction 13 is ^{89}Zr-DFO-PEG$_3$-Azepin-HSA seen at 14.0 minutes. The minor species, ^{89}Zr-DFO-PEG$_3$-Azepin is seen at 18.1 minutes.

The crude and G-100 purified ^{89}Zr-DFO-PEG$_3$-Azepin-HSA were analyzed by HPLC with UV/Radiation detection using a BioRad ENrich SEC 650 size exclusion column eluted with a PBS mobile phase, shown in Figure 14. The HPLC chromatogram of the crude reaction shows that the reaction did not completely form ^{89}Zr-DFO-PEG$_3$-Azepin-HSA. The percent photoconjugation was 55.0%. The HPLC of fraction 13 from the G-100 purification showed ^{89}Zr-DFO-PEG$_3$-Azepin-HSA as the major species with 6.5% of ^{89}Zr-DFO-PEG$_3$-Azepin. This demonstrates that the G-100 column does not completely separate ^{89}Zr-DFO-PEG$_3$-Azepin-HSA from the ^{89}Zr-DFO-PEG$_3$-Azepin.

Fractions 18, 19, and 31 from the G-100 purification were also analyzed by HPLC. The ratio of species within each fraction is presented in Table 1. Fraction 18 contained 85.7% HSA and 11.5% Azepin. Fraction 19 contained 84.6% HSA and 11.5% Azepin. Fraction 31 contained 6.4% HSA and 93.7% Azepin. As the fractions increased, the percent Azepin present increased.

The percent of HSA was similar in fractions 13 to 19, subsequently decreasing with increasing fractions.

Table 1: The ratio of species contained in the G-100 purified fractions of ^{89}Zr-DFO-PEG$_3$-Azepin-HSA.

Fraction	HSA (%)	Azepin (%)
13	78.9	6.5
18	85.7	11.5
19	84.6	12.0
31	6.4	93.7

^{89}Zr-DFO-PEG$_3$-Azepin-Cimzia

Cimzia was added to the ^{89}Zr-DFO-PEG$_3$-ArN$_3$ after radiolabeling and was irradiated for 15 minutes to produce ^{89}Zr-DFO-PEG$_3$-Azepin-Cimzia as a model antibody compound. The crude ^{89}Zr-DFO-PEG$_3$-Azepin-Cimzia was analyzed by HPLC with UV/Radiation detection using a Biosep 5mm SEC-s3000 290Å size exclusion column eluted with PBS mobile phase. Analysis of the radiation chromatogram seen in Figure 15 shows ^{89}Zr-DFO-PEG$_3$-Azepin-Cimzia at 11.8 minutes and ^{89}Zr-DFO-PEG$_3$-Azepin at 12.3 minutes. The amount of activity injected was not enough to provide a clear visualization of the distinct peaks, thus separation was difficult and the percent photoconjugation could not be determined.

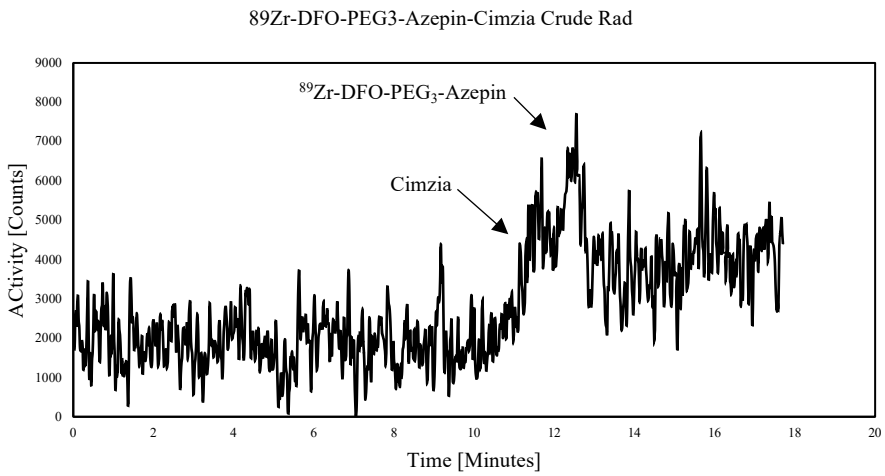

Figure 15: Rad chromatogram of crude ^{89}Zr-DFO-PEG$_3$-Azepin-Cimzia. The ^{89}Zr-DFO-PEG$_3$-Azepin-Cimzia is seen at 11.8 minutes and ^{89}Zr-DFO-PEG$_3$-Azepin seen at 12.3 minutes.

The crude reaction was purified through a PD-10 column using a PBS eluent and collected in 1mL fractions. An elution profile from a 2 mCi reaction was generated with the activity observed in each fraction, shown in Figure 16. It was observed that ^{89}Zr-DFO-PEG$_3$-Azepin-Cimzia reaction eluted in fractions 3 to 8. A majority of ^{89}Zr-DFO-PEG$_3$-Azepin-Cimzia eluted into fractions 4 to 6. Compared to the ^{89}Zr-DFO-PEG$_3$-Azepin, it appears that the labeled Cimzia and labeled Azepin may coelute in several fractions.

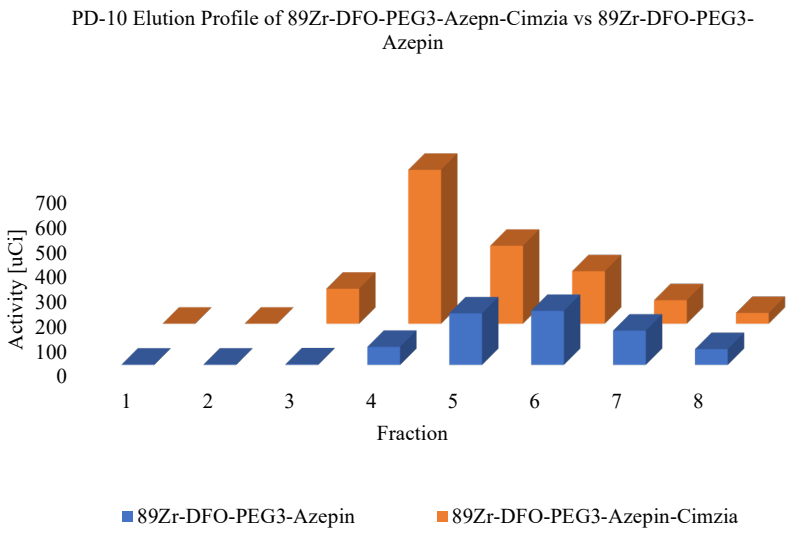

Figure 16: PD-10 fractions of ^{89}Zr-DFO-PEG$_3$-Azepin-Cimzia/^{89}Zr-DFO-PEG$_3$-Azepin. The elution profiles are compared to show the overlap of species in the ^{89}Zr-DFO-PEG$_3$-Azepin-Cimzia fractions.

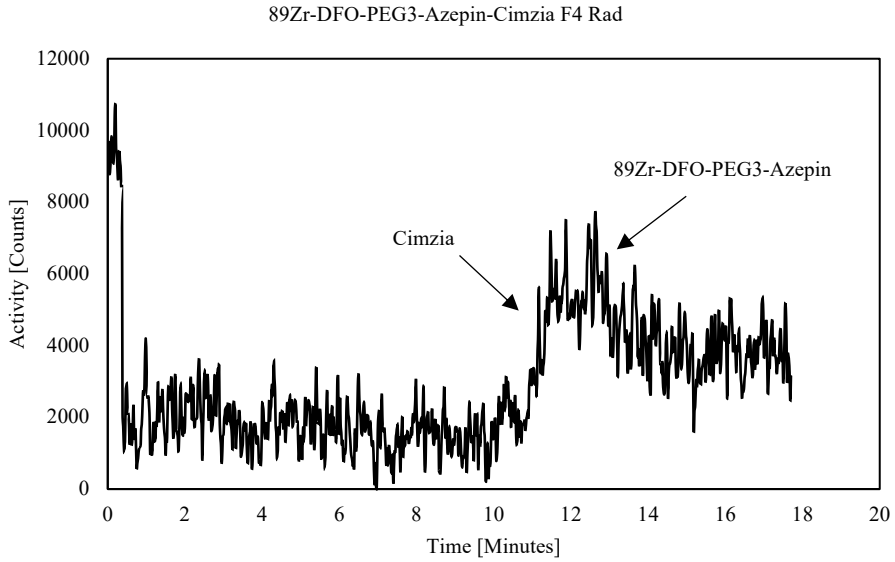

Figure 17: Rad chromatogram of ^{89}Zr-DFO-PEG$_3$-Azepin-Cimzia F4. The chromatogram shows a mixture of ^{89}Zr-DFO-PEG$_3$-Azepin-Cimzia and ^{89}Zr-DFO-PEG$_3$-Azepin.

The PD-10 purified ^{89}Zr-DFO-PEG$_3$-Azepin-Cimzia fraction 4 was analyzed by HPLC using a Biosep 5mm SEC-s3000 290Å size exclusion column eluted with a PBS mobile phase,

Figure 17. The amount of activity injected was not enough to determine radiochemical purity of the species.

A subsequent crude Cimzia reaction was purified through a Sephadex G-100 column using a PBS eluent and collected in 200 µL fractions. An elution profile, shown in Figure 18, of a 2 mCi reaction was generated. Two distinct peaks were observed with clear separation, the first peak between fractions 11 and 19, and the second between fractions 25 and 40.

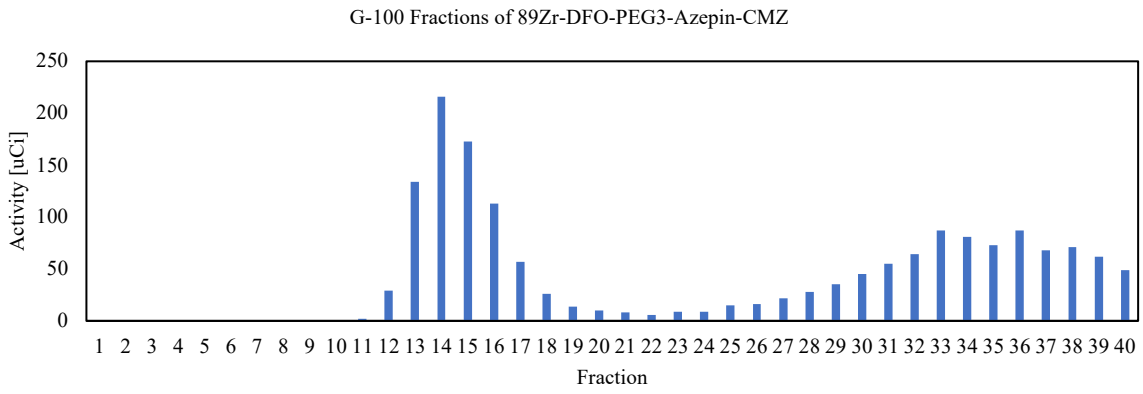

Figure 18: G-100 elution profile of ^{89}Zr-DFO-PEG$_3$-Azepin-Cimzia. There are two distinct peaks with clear separation between both. The first peak resides between fractions 11 and 19, and the second peak resides between fractions 25 and 40.

The crude and G-100 purified ^{89}Zr-DFO-PEG$_3$-Azepin-Cimzia fraction 14 were analyzed by HPLC using a BioRad ENrich SEC 650 size exclusion column eluted with a PBS mobile phase, shown in Figure 19. The HPLC chromatogram of the crude reaction shows that the reaction did not completely form ^{89}Zr-DFO-PEG$_3$-Azepin-Cimzia. The percent photoconjugation was 56.0%. The HPLC of fraction 14 from the G-100 purification showed 92.5% ^{89}Zr-DFO-PEG$_3$-Azepin-Cimzia at 11.2 minutes and 3.2% ^{89}Zr-DFO-PEG$_3$-Azepin at 18.1 minutes. This demonstrates that the G-100 column separated ^{89}Zr-DFO-PEG$_3$-Azepin-Cimzia from ^{89}Zr-DFO-PEG$_3$-Azepin to a better degree than the PD-10 purification.

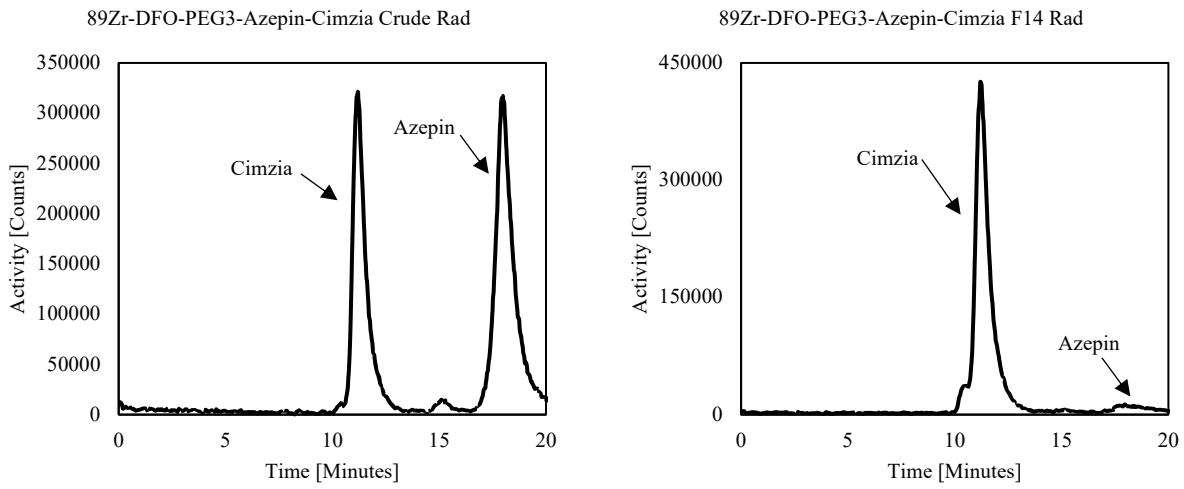

Figure 19: Rad chromatogram of crude and G-100 purified ^{89}Zr-DFO-PEG$_3$-Azepin-Cimzia. The radiation chromatograms of the crude ^{89}Zr-DFO-PEG$_3$-Azepin-Cimzia (left) and purified ^{89}Zr-DFO-PEG$_3$-Azepin-Cimzia fraction 14 (right). The major species in both the crude reaction and fraction 14 is ^{89}Zr-DFO-PEG$_3$-Azepin-Cimzia at 11.2 minutes. The minor species is ^{89}Zr-DFO-PEG$_3$-Azepin at 18.1 minutes in the crude reaction.

Fractions 17 and 33 were also analyzed by HPLC The ratio of species within each fraction is presented in Table 2. Fraction 17 contained 82.2% Cimzia and 11.2% Azepin. Fraction 33 only labeled Azepin.

Table 2: The ratio of species contained in the purified fractions of ^{89}Zr-DFO-PEG$_3$-Azepin-Cimzia.

Fraction	Cimzia (%)	Azepin (%)
14	92.5	3.2
17	82.2	11.2
33	0	100

^{89}Zr-DFO-PEG$_3$-Azepin-VRC01

VRC01 was added to the ^{89}Zr-DFO-PEG$_3$-ArN$_3$ and was irradiated for 15 minutes. The radiochemical purity of the crude ^{89}Zr-DFO-PEG$_3$-Azepin-VRC01 was analyzed by HPLC with UV/Radiation detection using a BioRad ENrich SEC 650 size exclusion column eluted with a PBS mobile phase, shown in Figure 20. Analysis of the radiation chromatogram shows 12.5%

^{89}Zr-DFO-PEG$_3$-Azepin-VRC01 at 12.9 minutes with the 5.5% aggregate at 11.8 minutes. The major species was unreacted ^{89}Zr-DFO-PEG$_3$-Azepin, 82% at 17.9 minutes.

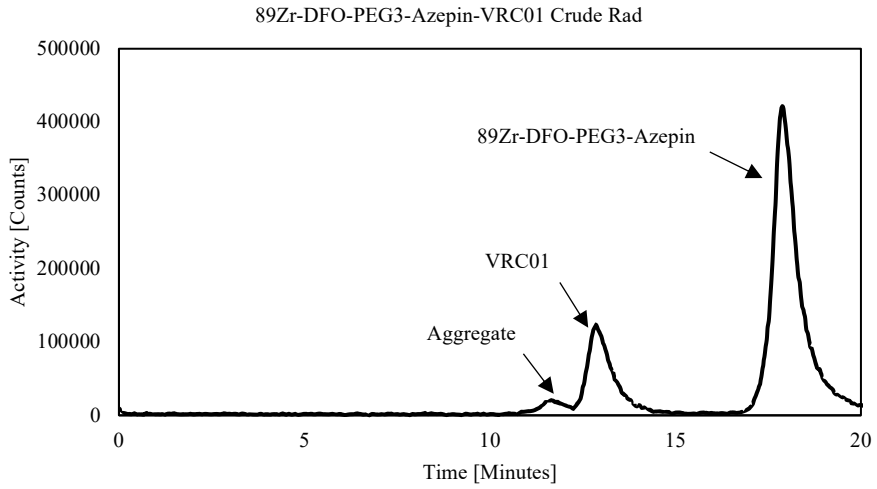

Figure 20: Rad chromatogram of ^{89}Zr-DFO-PEG$_3$-Azepin-VRC01. The major species is the ^{89}Zr-DFO-PEG$_3$-Azepin at 17.9 minutes. The minor species is ^{89}Zr-DFO-PEG$_3$-Azepin-VRC01 at 12.9 minutes with the aggregate at 11.8 minutes.

The crude reaction was purified through a Sephadex G-100 column using a PBS eluent and collected in 200 μL fractions. An elution profile, shown in Figure 21, from a 4 mCi reaction was generated. Two distinct peaks were observed, the first peak between fractions 11 and 17, and the second between fractions 22 and 40.

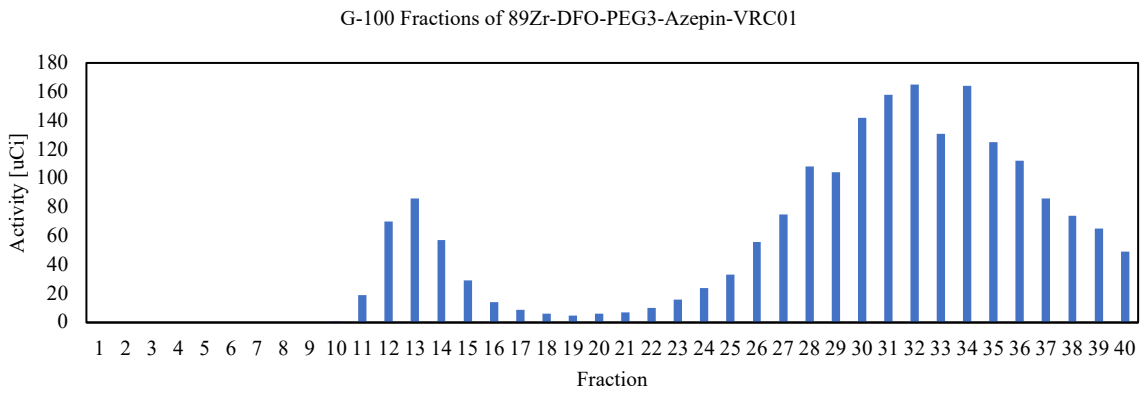

Figure 21: G-100 elution profile of ^{89}Zr-DFO-PEG$_3$-Azepin-VRC01. There are two distinct peaks with clear separation between both. The first peak resides between fractions 11 and 17, and the second peak resides between fractions 22 and 40.

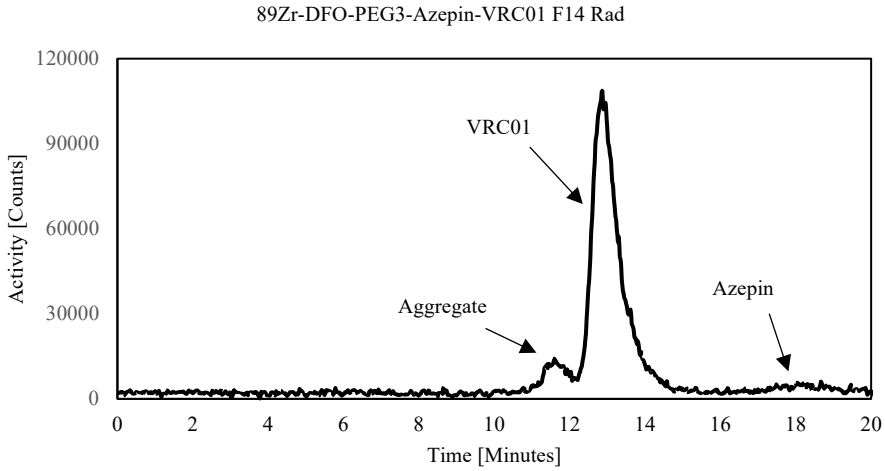

Figure 22: Rad chromatogram of ^{89}Zr-DFO-PEG$_3$-Azepin-VRC01 F14. The major species is ^{89}Zr-DFO-PEG$_3$-Azepin-VRC01 seen at 12.9 minutes with the aggregate at 11.8 minutes.

Figure 22 shows the radiation chromatogram for ^{89}Zr-DFO-PEG$_3$-Azepin-VRC01 fraction 14. The major species is 90% ^{89}Zr-DFO-PEG$_3$-Azepin-VRC01 seen at 12.9 minutes with the aggregate, 8.5% at 10.6 minutes. The minor species is 1.5% ^{89}Zr-DFO-PEG$_3$-Azepin at 17.9 minutes. This demonstrates the G-100 column could not completely separate ^{89}Zr-DFO-PEG$_3$-Azepin-VRC01 from ^{89}Zr-DFO-PEG$_3$-Azepin.

A binding assay was performed to assess the immunoreactivity of the labeled VRC01 by conducting eight five-fold dilutions of the purified ^{89}Zr-DFO-PEG$_3$-Azepin-VRC01 in triplicate. The diluted radiolabeled VRC01 was incubated with a RSC3 recombinant protein for two hours. The activity of extracted protein was measured on a Hidex gamma counter, and a binding curve was generated, shown in Figure 23. The dissociation constant of ^{89}Zr-DFO-PEG$_3$-Azepin-VRC01 was calculated as 0.4759 ± 0.0728 nM and R^2 = 0.9922.

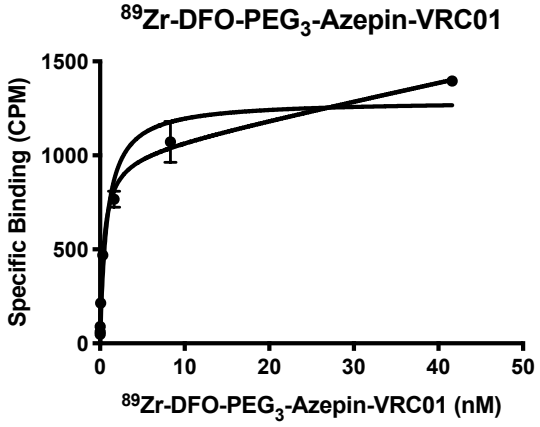

Figure 23: Biological activity assay of ^{89}Zr-DFO-PEG$_3$-Azepin-VRC01. The dissociation constant of ^{89}Zr-DFO-PEG$_3$-Azepin-VRC01 to a RSC3 recombinant protein. K_D for ^{89}Zr-DFO-PEG$_3$-Azepin-VRC01 is 0.4759 ± 0.0728 nM (n = 3, R^2 = 0.9922).

Discussion

The goal of the research project was to synthesize ^{89}Zr-DFO-PEG$_3$-Azepin-VRC01 using a one pot photoconjugation method and compare it to the conventional two-step method of synthesizing ^{89}Zr-DFO-VRC01 through the intermediate DFO-VRC01. The disadvantage of the conventional method of synthesis is that it requires the full characterization of the intermediate DFO-VRC01 conjugate before being radiolabeled with ^{89}Zr-oxalate. If the DFO-VRC01 conjugate fails any of the quality specifications, the conjugate must be resynthesized. Also the stability of the intermediate must be determined if it is a going to have a long shelf life. Unlike

the conventional method, the one-pot synthesis bypasses the need for a full characterization of an intermediate as the radiolabeling of the DFO-chelate and conjugation to the VRC01 occur sequentially, offering a streamlined process. It was also important to determine if the photoconjugation method affected the binding properties of VRC01, thus biological activity assays were performed with the tracers developed by both methods.

A. ^{89}Zr-DFO-PEG$_3$-Azepin-HSA

The light-induced one step synthesis of ^{89}Zr-DFO-PEG$_3$-Azepin-HSA was performed as a model protein compound to gain experience with the photoconjugation reaction. From the photoconjugation, it was observed that the reaction did not go to completion, therefore it was important to evaluate methods that would sufficiently separate the ^{89}Zr-DFO-PEG$_3$-Azepin-HSA from ^{89}Zr-DFO-PEG$_3$-Azepin. Efficient photoconjugation and good purification is critically important for the administration of the ^{89}Zr-DFO-PEG$_3$-Azepin-VRC01 to a patient as ^{89}Zr-DFO-PEG$_3$-Azepin in the final product would not pass quality testing.

Currently, size exclusion columns are used to purify crude reactions, separating high molecular weight species from low molecular weight species. With size exclusion PD-10 columns, the gel media used for the purification is Sephadex G-25, which provides a fractionation range of 1 kDA to 5 kDA for globular proteins. Any molecule that is larger than the fractionation range would be excluded from the gel pores and be eluted earlier. Any molecule below the fractionation range would be absorbed into the dextran pores, slowing the movement of the lighter molecules down the column, thus being eluted later. Therefore, any size exclusion column utilizing a similar gel media like G-25 for purification will typically elute the heaviest molecules first and the lightest molecules last. However, this elution profile is dependent on several factors such as uneven gel packing or uneven column loading. If the gel packing is

uneven such that one side of the column is tightly packed while the opposite side is loose, the molecules would have longer retention and better resolution on the thicker side whereas the loose side would not separate the species adequately, leading to coelutions of heavy and light molecules. With uneven column loading, one side may be eluted faster which would also lead to coelutions of large and small molecules.

With HSA having a molecular weight of around 66.5 kDa, finding a suitable method that would adequately separate ^{89}Zr-DFO-PEG$_3$-Azepin-HSA (MW: ~67 kDa) from ^{89}Zr-DFO-PEG$_3$-Azepin (MW: ~1.1 kDa) may provide a method that would work well or even better with the high molecular weight ^{89}Zr-DFO-PEG$_3$-Azepin-VRC01 (MW: ~150 kDa). The expected separation of the high molecular weight ^{89}Zr-DFO-PEG$_3$-Azepin-HSA from the lower molecular weight ^{89}Zr-DFO-PEG$_3$-Azepin by PD-10 column purification was not observed despite ^{89}Zr-DFO-PEG$_3$-Azepin being within the fractionation range. From the elution profile of the purified ^{89}Zr-DFO-PEG$_3$-Azepin-HSA seen in Figure 11, the labeled HSA was observed to elute into fractions 3 and 7, with overlap in the elution profile when compared to the profile of ^{89}Zr-DFO-PEG$_3$-Azepin. This indicated that ^{89}Zr-DFO-PEG$_3$-Azepin may have coeluted with ^{89}Zr-DFO-PEG$_3$-Azepin-HSA into the purified fractions which was later confirmed by HPLC analysis seen in Figure 12. However, the inability to adequately separate these two species provided incentive to explore a new purification column.

As an alternative to PD-10 columns, new columns were created using Sephadex G-100 powder. The fractionation range for globular proteins is 4 kDa to 150 kDa and is 1 kDa to 100 kDa for dextrans. The G-100 powder for purification was observed to give a distinct separation in the elution profile seen in Figure 13 between the ^{89}Zr-DFO-PEG$_3$-Azepin-HAS, seen in the earlier fractions, from ^{89}Zr-DFO-PEG$_3$-Azepin, seen in the later fractions. The radiation

chromatogram for fraction 13 in Figure 14 showed that the G-100 column used for purification was able to separate most of the ^{89}Zr-DFO-PEG$_3$-Azepin compared to the PD-10, showing only 6.5% of the ^{89}Zr-DFO-PEG$_3$-Azepin species within the purified fraction compared to 20%, which was a significant improvement in the ability to separate lower and higher molecular weight species. We hypothesized that for higher molecular weighted mAb/proteins, a greater or complete separation would be observed.

B. ^{89}Zr-DFO-PEG$_3$-Azepin-Cimzia

The synthesis of ^{89}Zr-DFO-PEG$_3$-Azepin-Cimzia was a model antibody compound due to Cimzia being readily available. The photoconjugation did not go to completion, with 56% ^{89}Zr-DFO-PEG$_3$-Azepin-Cimzia in the crude, seen in the HPLC analysis of Figure 19. In the PD-10 elution profile of ^{89}Zr-DFO-PEG$_3$-Azepin-Cimzia seen in Figure 16, ^{89}Zr-DFO-PEG$_3$-Azepin-Cimzia eluted into fractions 3 to 8, tailing off into the later fractions without a point of distinct separation. The radiation chromatogram of fraction 4 showed a mixture of both ^{89}Zr-DFO-PEG$_3$-Azepin-Cimzia and ^{89}Zr-DFO-PEG$_3$-Azepin, but due to the peaks occurring near baseline as a result of not enough injected activity, we were unable to determine the radiochemical purity. When purifying the crude ^{89}Zr-DFO-PEG$_3$-Azepin-Cimzia by G-100 column, a similar elution profile as seen with ^{89}Zr-DFO-PEG$_3$-Azepin-HSA was observed. The difference was that the fractions ^{89}Zr-DFO-PEG$_3$-Azepin-Cimzia eluted into had shifted to the left as a result of being a heavier molecule (MW: 91 kDa). SEC HPLC analysis of the purity of fraction 14, showed ^{89}Zr-DFO-PEG$_3$-Azepin still present in the fraction, but at a lower percent when compared to the ^{89}Zr-DFO-PEG$_3$-Azepin-HSA fraction 13. Still this method of separation was inadequate because it could not completely separate out ^{89}Zr-DFO-PEG$_3$-Azepin, but visually it was better than the purification of ^{89}Zr-DFO-PEG$_3$-Azepin-HSA.

C. ^{89}Zr-DFO-PEG$_3$-Azepin-VRC01

The synthesis of ^{89}Zr-DFO-PEG$_3$-Azepin-VRC01 was the primary antibody compound for the evaluation of the photoconjugation method. The photoconjugation did not go to completion, with 12.5% ^{89}Zr-DFO-PEG$_3$-Azepin-VRC01 in the crude, seen in the HPLC analysis of Figure 20. From the G-100 column fractionation study in Figure 21, ^{89}Zr-DFO-PEG$_3$-Azepin-VRC01 eluted into the earlier fractions as expected after the studies conducted with HSA and Cimzia. When determining the radiochemical purity in Figure 14, it was observed that 1.5% of ^{89}Zr-DFO-PEG$_3$-Azepin was still present. Although G-100 showed a significant improvement in the separation between higher and lower molecular weight species, it was still unable to completely separate ^{89}Zr-DFO-PEG$_3$-Azepin-VRC01 from ^{89}Zr-DFO-PEG$_3$-Azepin. Due to the residual ^{89}Zr-DFO-PEG$_3$-Azepin still present, it would be challenging to release the product for injection into humans.

It was important to determine if the photoconjugation method affected the binding properties of VRC01, thus binding assays were performed to determine the immunoreactivity of ^{89}Zr-DFO-PEG$_3$-Azepin-VRC01 and ^{89}Zr-DFO-VRC01. The dissociation constant of ^{89}Zr-DFO-PEG$_3$-Azepin-VRC01 and ^{89}Zr-DFO-VRC01 binding to RSC3 recombinant protein was in the 0.4-20 nM range. This is comparable to the value of 5 nM seen for VRC01 binding.[14] This is significant because this binding assay showed that the photoconjugation method for the synthesis of the tracer did not affect the binding properties, immunoreactivity, of the VRC01.

There are several challenges that we have discovered from the photoconjugation synthesis. The first is that the synthesis does not go to completion, therefore we must perform a purification. In the future, we want to optimize the conditions of the synthesis that would increase the photoconjugation conversion, minimizing the amount of ^{89}Zr-DFO-PEG$_3$-Azepin in

the reaction that needs to be purified. The second is that from size exclusion purification, there was insufficient separation of the ^{89}Zr-DFO-PEG$_3$-Azepin-mAb/protein from ^{89}Zr-DFO-PEG$_3$-Azepin. To optimize separations in the future, we would explore increasing the length of the column or new separation resins.

Conclusion

The light-induced one pot method was successful in synthesizing ^{89}Zr-DFO-PEG$_3$-Azepin-VRC01. It was possible to obtain a better visualization of the separation between ^{89}Zr-DFO-PEG$_3$-Azepin-VRC01 and ^{89}Zr-DFO-PEG$_3$-Azepin using a new size exclusion HPLC column with no overlap between higher and lower molecular weight species. The development of a new SEC purification column using Sephadex G-100 powder allowed for an optimal separation of ^{89}Zr-DFO-PEG$_3$-Azepin-VRC01 from ^{89}Zr-DFO-PEG$_3$-Azepin with purity higher than 99%. From the binding assay, the ^{89}Zr-DFO-PEG$_3$-Azepin-VRC01 showed efficient binding to the gp120 protein on RSC3 when compared to the ^{89}Zr-DFO-VRC01 binding assay, indicating that the photoconjugation method did not affect the binding properties of VRC01.

References

1. Guillou, A., Earley, D. F., Klingler, S., Nisli, E., Nüesch, L. J., Fay, R., & Holland, J. P. (2021). The influence of a polyethylene Glycol linker on the metabolism and pharmacokinetics of a ^{89}Zr-Radiolabeled Antibody. Bioconjugate Chemistry, 32(7), 1263–1275. https://doi.org/10.1021/acs.bioconjchem.1c00172
2. Guillou, A., Earley, D. F., Patra, M., & Holland, J. P. (2020). Light-induced synthesis of protein conjugates and its application in photoradiosynthesis of ^{89}Zr-radiolabeled monoclonal antibodies. Nature Protocols, 15(11), 3579-3594.https://doi.org/10.1038/s41596-020-0386-5
3. Wu, A. M. (2008). Antibodies and Antimatter: The Resurgence of Immuno-PET. Journal of Nuclear Medicine, 50(1), 2–5. https://doi.org/10.2967/jnumed.108.056887
4. Ryman, J. T., & Meibohm, B. (2017). Pharmacokinetics of Monoclonal Antibodies. CPT: Pharmacometrics & Systems Pharmacology, 6(9), 576–588. https://doi.org/10.1002/psp4.12224
5. Ovacik, M., & Lin, K. (2018). Tutorial on Monoclonal Antibody Pharmacokinetics and Its Considerations in Early Development. Clinical and Translational Science, 11(6), 540–552. https://doi.org/10.1111/cts.12567
6. Chang, A. J., DeSilva, R., Jain, S., Lears, K., Rogers, B., & Lapi, S. (2012). ^{89}Zr-Radiolabeled Trastuzumab Imaging in Orthotopic and Metastatic Breast Tumors. Pharmaceuticals, 5(1), 79–93. doi:10.3390/ph5010079
7. Zhang, Y., Hong, H., & Cai, W. (2011). PET tracers based on Zirconium-89. Current Radiopharmaceuticals, 4(2), 131–139. https://doi.org/10.2174/1874471011104020131
8. Zeglis, B. M., & Lewis, J. S. (2015). The Bioconjugation and Radiosynthesis of ^{89}Zr-DFO-labeled Antibodies. Journal of Visualized Experiments, (96). https://doi.org/10.3791/52521

9. Vosjan, M. J., Perk, L. R., Visser, G. W., Budde, M., Jurek, P., Kiefer, G. E., & van Dongen, G. A. (2010). Conjugation and radiolabeling of monoclonal antibodies with zirconium-89 for pet imaging using the bifunctional chelate p-isothiocyanatobenzyl-desferrioxamine. Nature Protocols, 5(4), 739–743. https://doi.org/10.1038/nprot.2010.13
10. UCSF Radiopharmaceutical Facility. (2019). Manufacturing Instructions - ^{89}Zr-DFO-VRC01 (SOP M961).
11. CFR - Code of Federal Regulations Title 21. accessdata.fda.gov. (n.d.). https://www.accessdata.fda.gov/scripts/cdrh/cfdocs/cfcfr/CFRSearch.cfm?CFRPart=212&showFR=1&subpartNode=21%3A4.0.1.1.12.8.
12. Niu, G., Lang, L., Kiesewetter, D. O., Ma, Y., Sun, Z., Guo, N., Guo, J., Wu, C., & Chen, X. (2014). In Vivo Labeling of Serum Albumin for PET. Journal of Nuclear Medicine, 55(7), 1150–1156. https://doi.org/10.2967/jnumed.114.139642
13. Beckford-Vera, D.R., Gonzalez-Junca, A., Janneck, J.S. et al. PET/CT Imaging of Human TNFα Using [^{89}Zr]Certolizumab Pegol in a Transgenic Preclinical Model of Rheumatoid Arthritis. Mol Imaging Biol 22, 105–114 (2020). https://doi.org/10.1007/s11307-019-01363-0
14. Zhou, T., Georgiev, I., Wu, X., Yang, Z.-Y., Dai, K., Finzi, A., Do Kwon, Y., Scheid, J. F., Shi, W., Xu, L., Yang, Y., Zhu, J., Nussenzweig, M. C., Sodroski, J., Shapiro, L., Nabel, G. J., Mascola, J. R., & Kwong, P. D. (2010). Structural Basis for Broad and Potent Neutralization of HIV-1 by Antibody VRC01. Science, 329(5993), 811–817. https://doi.org/10.1126/science.1192819
15. Ledgerwood, J. E., Coates, E. E., Yamshchikov, G., Saunders, J. G., Holman, L., Enama, M. E., DeZure, A., Lynch, R. M., Gordon, I., Plummer, S., Hendel, C. S., Pegu, A., Conan-

Cibotti, M., Sitar, S., Bailer, R. T., Narpala, S., McDermott, A., Louder, M., O'Dell, S., … Graham, B. S. (2015). Safety, Pharmacokinetics and Neutralization of the Broadly Neutralizing HIV-1 Human Monoclonal Antibody VRC01 in Healthy Adults. Clinical & Experimental Immunology, 182(3), 289–301. https://doi.org/10.1111/cei.12692

16. Beckford-Vera, D. R., Flavell, R. R., Seo, Y., Martinez-Ortiz, E., Aslam, M., Thanh, C., Fehrman, E., Pardons, M., Kumar, S., Deitchman, A. N., Ravanfar, V., Schulte, B., Wu, I. K, Pan, T., Nixon, C. C., Iyer, N. S., Torres, L., Munter, S. E., Hyunh, T., Petropoulos, C. J., Hoh, R., Franc, B., Gama, L., Koup, R. A., Mascola, J. R., Chomont, N., Deeks, S. G., VanBrocklin, H. F., Henrich, T. J. First-in-human ImmunoPET Imaging of HIV-1 Infection using ^{89}Zr-labeled VRC01. Nature Communications, Submitted.

Publishing Agreement

It is the policy of the University to encourage open access and broad distribution of all theses, dissertations, and manuscripts. The Graduate Division will facilitate the distribution of UCSF theses, dissertations, and manuscripts to the UCSF Library for open access and distribution. UCSF will make such theses, dissertations, and manuscripts accessible to the public and will take reasonable steps to preserve these works in perpetuity.

I hereby grant the non-exclusive, perpetual right to The Regents of the University of California to reproduce, publicly display, distribute, preserve, and publish copies of my thesis, dissertation, or manuscript in any form or media, now existing or later derived, including access online for teaching, research, and public service purposes.

DocuSigned by:
Cyril Fong
B183835D4DD8477...
Author Signature

8/31/2021
Date